Brief Communication

MOLECULAR METABOLISM

Fibroblast growth factor 19 stimulates water intake

José Ursic-Bedoya [1,2,5], Carine Chavey [1,5], Guillaume Desandré [1], Lucy Meunier [1,2], Anne-Marie Dupuy [3], Iria Gonzalez-Dopeso Reyes [1], Thierry Tordjmann [4], Eric Assénat [1,2], Urszula Hibner [1], Damien Gregoire [1,*]

ABSTRACT

Fibroblast growth factor 19 (FGF19) is a hormone with pleiotropic metabolic functions, leading to ongoing development of analogues for treatment of metabolic disorders. On the other hand, FGF19 is overexpressed in a sub-group of hepatocellular carcinoma (HCC) patients and has oncogenic properties. It is therefore crucial to precisely define FGF19 effects, notably in the context of chronic exposure to elevated concentrations of the hormone. Here, we used hydrodynamic gene transfer to generate a transgenic mouse model with long-term FGF19 hepatic overexpression. We describe a novel effect of FGF19, namely the stimulation of water intake. This phenotype, lasting at least over a 6-month period, depends on signaling in the central nervous system and is independent of FGF21, although it mimics some of its features. We further show that HCC patients with high levels of circulating FGF19 have a reduced natremia, indicating dipsogenic features. The present study provides evidence of a new activity of FGF19, which could be clinically relevant in the context of FGF19 overexpressing cancers and in the course of treatment of metabolic disorders by FGF19 analogues.

Keywords Liver; FGFR4; Hepatocellular carcinoma; Hydrodynamic gene transfer; Endocrine

1. INTRODUCTION

Fibroblast growth factor 19, FGF19 (and its mouse ortholog, FGF15), functions as a hormone, notably controlling bile acids synthesis and nutrient metabolism [1]. FGF15/19 has been reported to exert multiple effects in the regulation of glucose and lipid metabolism, as well as in energy expenditure and body adiposity, through its actions on liver, muscle, white adipose tissue and brain [2].

Under physiological conditions, FGF19 is expressed in the post-prandial phase by enterocytes of the terminal ileum [3]. The expression by hepatocytes has also been described in cholestasis [4–6]. FGF19 belongs to the endocrine FGF subfamily, along with FGF21 and FGF23. Endocrine FGF lack the heparin binding domain found in canonical FGFs and act through the binding to a FGF receptor (FGFR 1 to 4) in complex with a co-receptor, β-klotho (KLB) for FGF19 and FGF21 [7,8]. While many of the FGF19 activities are thought to be mediated by FGFR4/KLB signaling, FGF19 and FGF21 also display overlapping metabolic regulations through activation of FGFR1c/KLB signaling [9], notably in the hypothalamus [10,11]. Because of their metabolic effects, FGF19 and FGF21 pathways are considered as promising therapeutic targets for several diseases [12]. In particular, FGF19 has generated a great interest in pharmacological research for treatment of chronic liver diseases such as nonalcoholic steatohepatitis [13,14], primary biliary cholangitis [15] and primary sclerosing cholangitis [16].

On top of its metabolic effects, FGF19/FGFR4 pathway shows oncogenic functions in several cancers, notably in hepatocellular carcinoma, the most frequent primary liver cancer. The 11q13.3 genomic region containing FGF19 is frequently amplified in HCC tumors (4–15%) [17–19], and overexpression of FGF19 independently of amplification has also been reported [20,21]. Moreover, HCC patients display higher circulating levels of FGF19 than control population [22]. These findings led to the development of potent and selective FGFR4 inhibitors, as well as monoclonal antibodies [23,24], which are currently tested in clinical trials for FGF19-driven hepatocarcinoma, underscoring the therapeutic promise of targeting the FGF19 pathway in HCC [25].

Because of these paradoxical effects on metabolism and oncogenesis, it is crucial to better delineate the complex interplay of FGF19 roles and actions. In this study, we generated a mouse model of FGF19 overexpression by hepatocytes, and identified a new metabolic effect of

[1]Institut de Génétique Moléculaire de Montpellier, University of Montpellier, CNRS, Montpellier, France [2]Department of Hepatogastroenterology, Hepatology and Liver Transplantation Unit, Saint Eloi Hospital, University of Montpellier, France [3]Biochemistry and Hormonology Department, Lapeyronie Hospital, University of Montpellier, Montpellier, France [4]Université Paris Saclay, Faculté des Sciences d'Orsay, INSERM U.1193, Bât. 443, 91405, Orsay, France

[5] Co-first authorship.

*Corresponding author. Institut de Génétique Moléculaire de Montpellier, 1919, route de Mende, 34293 Montpellier Cedex, France. E-mail: damien.gregoire@igmm.cnrs.fr (D. Gregoire).

Abbreviations: FGF19, fibroblast growth factor 19; HCC, hepatocellular carcinoma; HGT, hydrodynamic gene transfer; FGFR, fibroblast growth factor receptor; FGF15, fibroblast growth factor 15; KLB, β-klotho; HPRT, hypoxanthine phospho-ribosyltransferase; SB100X, Sleeping Beauty transposase 100X; FXR, farnesoid X receptor; BCLC, Barcelona clinic liver cancer; Meld, Model for end stage liver disease

Received December 17, 2021 • Revision received March 18, 2022 • Accepted March 27, 2022 • Available online 31 March 2022

https://doi.org/10.1016/j.molmet.2022.101483

FGF19, namely the stimulation of water intake. We further report that HCC patients with increased circulating FGF19 concentrations show features of disturbance of the hydrosodic balance.

2. METHODS

2.1. Vectors: cloning of FGF19/15

Plasmids constructs pSBbi-RN-FGF19 and pSBbi-BB-FGF15 were generated by cloning the human FGF19, amplified from Huh7 cDNA, and the murine FGF15, amplified from C57Bl/6J mouse ileum cDNA, into psBbi-RN and psBbi-BB plasmids (gifts from Eric Kowarz, Addgene plasmid #60519 and #60521, respectively), previously digested by the restriction enzyme SfiI. Primer sets for amplification of the inserts (with SfiI recognition site):

FGF19-SfiI-for-5′-ATCGGGCCTCTGAGGCCCAGGGAGGTGCCATGCGGA-3′

FGF19-SfiI-rev-5′-CGATGGCCTGACAGGCCGCCCCTGGCAGCAGTGAAGA-3′

FGF15-SfiI-for-5′-ATCGGGCCTCTGAGGCCCCCGAGGTGTCATGGCGAG-3′

FGF15-SfiI-rev-5′-CGATGGCCTGACAGGCCCGGAATCCTGTCATTTCTG-3′

FGF19dCTD sequence, described by Wu. et al. [26] was amplified from the ORF sequence of FGF19 (residues 1 to 177, including the peptide signal) and the SfiI restriction sites were added using the primer forward (5′-ATCGGGCCTCTGAGGCCATGCGGAGCGGGTGTGTG-3′) and reverse (5′-CGATGGCCTGACAGGCCCTA-CTCAGGCTCCTCTGGGAC-3′). The amplicon was then cloned onto the pSBbi-RN vector (addgene plasmid #60519) linearized using the SfiI restriction enzyme.

2.2. Animal models

All reported animal procedures were carried out in accordance with the rules of the French Institutional Animal Care and Use Committee and European Community Council (2010/63/EU). Animal studies were approved by institutional ethical committee (Comité d'éthique en expérimentation animale Languedoc-Roussillon (#36)) and by the Ministère de l'Enseignement Supérieur, de la Recherche et de l'Innovation (Apafis #10278-2018082809241782v1, Apafis #32384-2021070917596346 v2).

Hydrodynamic Gene Delivery**:** Hydrodynamic injections were performed in 6—8 week-old C57Bl/6J female (unless stated otherwise) mice, as described previously [27,28]. Briefly, 0.1 mL/g body weight of a solution of sterile saline containing plasmids of interest were injected into lateral tail vein over 8—10 s psBBi-FGF19-dTomato (12.5 μg), psBBi-dTomato (12.5 μg), psBBi-FGF15-mTagBFP (12.5 μg) or psBBi-mTagBFP (12.5 μg) were injected together with sleeping beauty transposase SB100X (2.5 μg, ratio of 5:1). pCMV(CAT)T7-SB100 was a gift from Zsuzsanna Izsvak (Addgene plasmid #34879).

Allografts: C57Bl/6J female mice (Charles River) mice were anesthetized with intra-peritoneal injection of Xylazine-Ketamine mixture. After incision of abdominal wall and peritoneum, the left lateral lobe of the liver was pulled out of the mouse body. 5000 cells, resuspended in 5 μL of 25% Matrigel (BD) - PBS, were injected using a 10 μL Hamilton syringe in the left lobe of the liver. After injection, liver was put back in normal position and the abdomen was sutured. Mice were monitored daily during 3 weeks, then euthanized before the tissues were collected and fixed following classical procedures.

2.3. Water consumption experiments

Water consumption was measured by weighing the bottles of the cages [29,30] three times a week, and daily water intake was normalized by mean body weight of animals in each cage (n = 2—5 mice/cage). For the double bottle assay, mice were acclimated to cages with two bottles containing water for one week. They were then given access to bottles, one containing water with 3% sucrose (Sigma-Aldrich #16104) and another pure water. Water and water-3% sucrose intake was measured every two days. The position of bottles was changed every two days. Acute water loading was performed by an intraperitoneal injection of 2 mL of water. Mice were immediately placed in individual cages without access to either food or water. Urine was collected hourly over 6 h. To measure the 24 h cumulative urine output, mice were housed in individual metabolic cages with ad libitum access to water and food. Mice were acclimated for 24 h before starting the experiment for 3 days. Osmolality were measured on the 24 h-total urine output.

Food intake and body weight were measured once per week over a period of one month. Daily food consumption was calculated after normalization by the body weight.

2.4. Blood samples for ELISA experiments

Mice were fasted for 4—6 h then killed by anesthetic overdose with isoflurane. Blood was collected by intracardiac puncture and plasma purified by centrifugation. Plasma FGF19, FGF19$^{\Delta CTD}$ and FGF21 were measured by ELISA, according to the manufacturers' instructions: human FGF19 ELISA kit (Biovendor, RD191107200R), mouse FGF21 ELISA kit (Sigma-Aldrich, EZRMFGF21-26K).

2.5. Bile samples and bile acid pool composition

Mice were fasted for 4—6 h then bile was collected by gallbladder puncture following animal euthanasia. Bile acids measurements were performed on mouse bile by high performance liquid chromatography-tandem mass spectrometry as previously described [31].

2.6. RNA isolation, qPCR

RNA was extracted from liver tissue and purified using RNeasy mini kit (Qiagen) according to manufacturer's protocol. Reverse transcription of total RNA (1 μg) was done with QuantiTect Reverse Transcription kit (Qiagen), and cDNA quantified using LC Fast start DNA Master SYBR Green I Mix (Roche) with primers detailed below on LightCycler480 apparatus (Roche). Gene expression levels were normalized with hypoxanthine phospho-ribosyltransferase (HPRT). Primer pairs used for qPCR:

Hprt 5′- GCAGTACAGCCCCAAAATGG-3′ and 5′-GGTCCTTTTCACCAGCAAGCT-3′

FGF19 5′-CCAGATGGCTACAATGTGTACC-3′ and 5′-CAGCATGGGCAGGAAATGA-3′

Cyp7a1 5′-CTGCAACCTTCTGGAGCTTA-3′ and 5′-ATCTAGTACTGGCAGGTTGTTT-3′

Cyp8b1 5′- CCTGTTTCTGGGTCCTCTTATTC-3′ and 5′-TCTCCTCCATCACGCTGTC-3'

Fgf15 5′-TGTCAGATGAAGATCCACTCTTTCTCTA-3′ and 5′-GGATTCGGAGGAAGCAGTTG-3'

2.7. Human studies

A total of 173 patients from the prospective HCC "Liverpool" cohort conducted in the Montpellier University Hospital were included and analyzed retrospectively. All patients provided written consent for research at the time of their blood collection, in line with international regulations and ICH GCP (International Conference on Harmonization- Good Clinical Practice, Biobank Registration Number DC 2014-2328 AC 2014-2335). Montpellier University Hospital Institutional Review Board committee approved this study (N°

2019_IRB-MTP_01-11). All the patients had FGF19 plasma concentration measured at the inclusion using human FGF19 ELISA kit (Biovendor, RD191107200R), according to the manufacturers' instructions. Meld Na score was calculated with the formula described in the princeps article [32].

2.8. Statistical analyses

Data sets were tested with 2-tailed unpaired Student *t* tests or Mann-Whitney U tests, correlations were analyzed with Pearson's χ^2 test using Prism Software version 8 (GraphPad). Significant *P* values are shown as: $^{*}P < 0.05$, $^{**}P < 0.01$, $^{***}P < 0.001$, and $^{****}P < 0.0001$. Comparisons of the mRNA expression levels between groups were assessed using Mann-Whitney U test. Spearman's rank-order correlation was used to test the association between continuous variables. Univariate survival analysis was performed using Kaplan-Meier curve with log-rank test.

3. RESULTS

3.1. Mouse model of FGF19 expression

We used hydrodynamic gene transfer (HGT) technique [28,33] to generate a mouse model in which FGF19 is overexpressed by a fraction of hepatocytes. The rapid injection of a large volume of solution (10% w/v) in the tail vein leads to *in vivo* transfection of hepatocytes. Combination of plasmids encoding the Sleeping Beauty transposase SB100X and FGF19 was used to establish stable expression of the human hormone (Figure 1A). We routinely detected by epifluorescence microscopy one to two percent of transfected hepatocytes, which persisted up to 6 months after the injection (Figure 1B). The long-term expression of the transgene was confirmed by RT-qPCR analysis (Figure 1C). The level of FGF19 in plasma, detected by ELISA, was around 10 ng/mL ($CI_{95\%} = [3.5-15.0]$) two weeks post-transfection and remained high, despite its gradual decrease, to reach 1 ng/mL

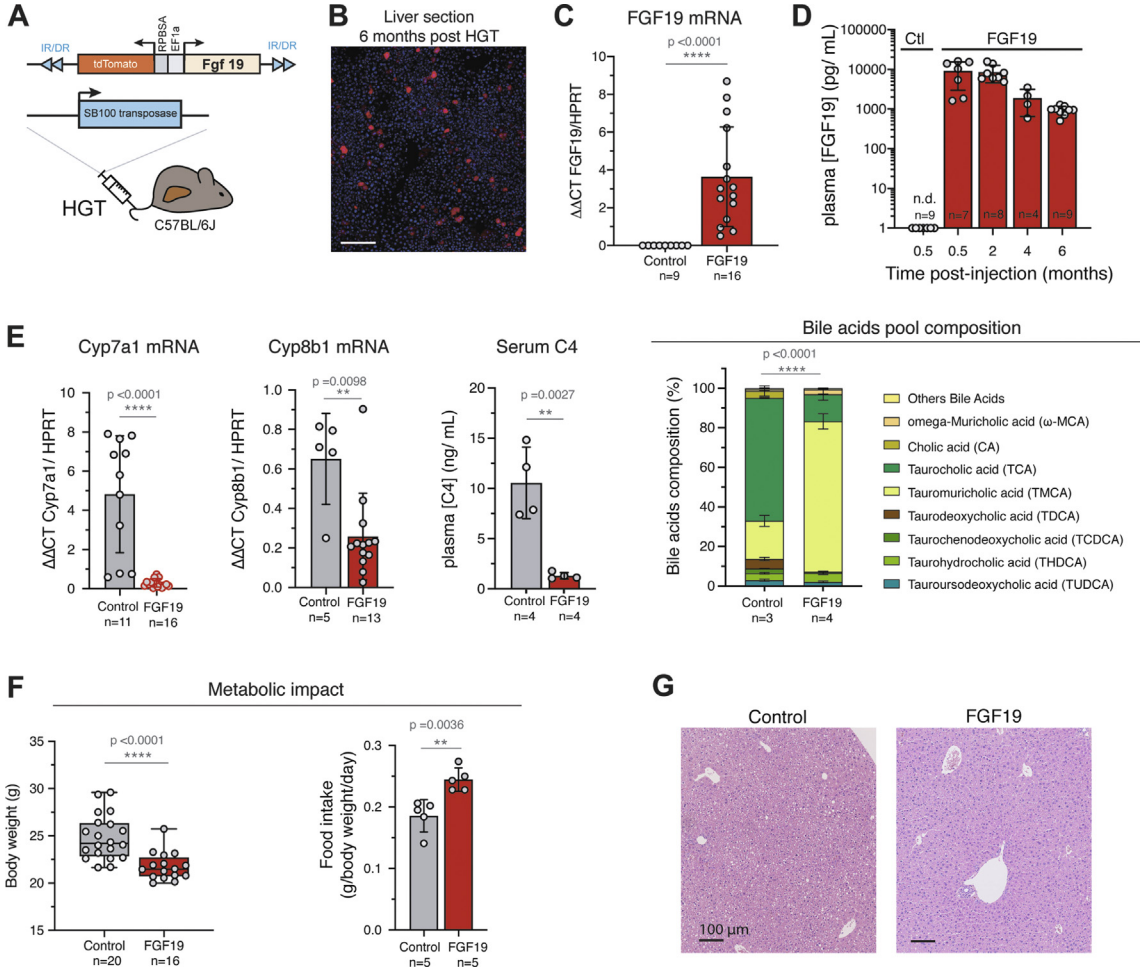

Figure 1: In vivo stable transfection of hepatocytes with FGF19 leads to long term secretion of biologically active FGF19. A. Mouse model strategy based on hydrodynamic gene transfer (HGT). Empty vector expressing only dTomato («Control») are used as control. **B**. Cryosection of liver 6 months after HGT, showing stably transfected hepatocytes that express dTomato. Scale bar: 100 µm. **C.** qPCR quantification of FGF19 mRNA in control and FGF19 transfected livers 6 months post injection. Plasmids combined with transposase used for HGT are indicated: control-dTomato («Ctl») and FGF19-dTomato («FGF19»). Data are presented as mean ± SD. Mann-Whitney test p-values are shown. **D.** Plasma levels of FGF19 detected by ELISA. The number of mice analyzed for each time point is indicated. Data are presented as mean ± SD, with statistical significance of Mann-Whitney test shown. **E**. qPCR quantification of mRNA expression of Cyp7a1 and Cyp8b1, target genes of FGF19/FGFR4 pathway; Serum 7 α-hydroxy-4-cholesten-3-one (C4) levels, serum biomarker of bile acid synthesis and biliary bile acids pool composition. All data are presented as mean ± SD. Unpaired Student's t-test p-values and significance are shown unless for bile acids composition, for which two-way ANOVA test significance is shown. **F.** Body weight of control and FGF19 HGT mice at 6 months (left panel). Food intake of control and FGF19 HGT mice first month following HGT (right panel). Data are presented as mean ± SD. Unpaired Student's t-test p-values and significance are shown. **G**. HES staining of liver sections of control and FGF19 HGT mice after 6 months, showing no visible alteration on liver morphology. $^{*}p \leq 0.05$, $^{**}p < 0.01$, $^{***}p < 0.001$, $^{****}p < 0.0001$. N.s: not significant. n. d: not detectable.

at 6 months post-injection ($CI_{95\%}$ = [0.76—1.11]) (Figure 1D) [34—36]. These concentrations are supra-physiological, as healthy human subjects display circulating concentrations of 50—590 pg/mL [1]; however, they are close to those observed in a subset of HCC patients [22]. Of note, these pathologically relevant concentrations are 100 to 1000-fold lower than to those reported in a model of AAV infection (1 μg/mL [37]). FGF19-expressing mice showed the previously characterized transcriptional repression of *Cyp7a1* and *Cyp8b1*, key enzymes of bile acids synthesis from cholesterol (Figure 1E). Serum 7α-hydroxy-4-cholesten-3-one (C4) level, a biomarker of bile acid synthesis, was also significantly reduced on FGF19-expressing mice (Figure 1E, 10.6 ng/mL $CI_{95\%}$ = [4.9; 16.2] for controls *vs* 1.3 ng/mL $CI_{95\%}$ = [0.8; 1.8] for FGF19, p = 0.0027). The composition of the bile acids pool in the FGF19-expressing animals was indicative of the inhibition of the classical pathway of bile acids synthesis, accompanied by a stimulation of the alternative pathway (Figure 1E, right panel, and Supplementary Fig. 1). In agreement with previous reports [10,36], FGF19 had a significant effect on metabolic rate, as indicated by a decrease of the body weight despite increase in food intake (Figure 1F). Histological analysis of livers revealed no visible effect of FGF19 overexpression (Figure 1G). Altogether, these results indicate that the secreted FGF19 is active, and that the circulating levels are compatible with its physiological functions.

3.2. FGF19 overexpression increases water intake

While studying metabolic effects in FGF19 transgenic mice, we serendipitously observed that their cages were very wet compared to those of control mice, suggesting increased urine production. This prompted us to measure the animals' water intake. We observed that FGF19 expressing mice drank 6.6—7.8 mL/day ($CI_{95\%}$ of the mean) compared to 2.9—3.1 mL/day for control animals hydrodynamically injected with an empty vector ($CI_{95\%}$ = [0.32; 0.39] vs $CI_{95\%}$ = [0.15; 0.17] mL/day/g after normalization by body weight; p-value <0.0001) (Figure 2A and Supplementary Fig. 2). Strikingly, this phenotype was stable in time for at least 5 months. The increase of water intake was associated with a significant decrease of urine osmolality (Figure 2B, 1744 mOsm/kg/H_20 $CI_{95\%}$ = [1512; 1976] for controls *vs* 723 mOsm/kg/H_20 $CI_{95\%}$ = [568; 879] for FGF19, p < 0.0001). Measuring urine production in individual metabolic cages showed that $FGF19^+$ mice have an increased urine output compared to controls (Figure 2C, 490 μL/day $CI_{95\%}$ = [204; 775] for controls *vs* 2871 μL/day $CI_{95\%}$ = [1589; 4153] for FGF19, p = 0.0003) and confirmed the phenotype of decreased urine osmolality (Figure 2D). Altogether, these results indicate that FGF19 overexpression mimics a phenotype of diabetes insipidus.

Next, we assessed the effect of FGF19 overexpression on water drinking in another experimental system, in which FGF19 is produced by hepatic tumor cells. To model FGF19-negative and FGF19-positive hepatic tumors, we implanted intrahepatic allografts of oncogenic cell lines derived from Myc-sgTrp53 or Myc-sgTrp53-FGF19 tumors. Both cell lines were driven by c-Myc oncogene in conjunction with inactivation of the p53 tumor suppressor, associated for the latter with FGF19 expression. Whereas Myc-sgTrp53 tumor development had no impact on water intake, mice injected with FGF19-expressing cells showed progressive rise of water intake from 0.1 to 0.2 mL/day/g body weight as tumors grew (Figure 2E and Supplementary Fig. 2). Mean circulating FGF19 levels at 3 weeks in mice injected with Myc-sgTrp53-FGF19 cells were high: 153 ng/mL ($CI_{95\%}$ = [81; 225]), approaching those obtained with AAV-driven FGF19 liver overexpression [37]. Thus, FGF19-driven increase of water intake by FGF19 was confirmed in a second experimental model. Importantly, this phenotype might be relevant for the subset of HCC patients overexpressing FGF19. It is unclear why the drinking phenotype has not been previously described in FGF19 overexpressing mice [37,38]. We note, however, that it would have probably escaped our notice if we were not directly handling the cages.

To determine if the diabetes insipidus phenotype was sex dependent, we next overexpressed FGF19 by HGT in C57Bl/6J males. Again, the FGF19 expression increased water intake, leading to a mean water consumption of 0.31 mL/day/g body weight (CI95% = [0.24; 0.37]) during the first month after HGT (Figure 2F). We next investigated whether the overexpression of FGF15, the FGF19 mouse ortholog, also gave rise to the water drinking phenotype. Hydrodynamic gene transfer of FGF15 encoding plasmid led to levels of hepatic expression indistinguishable from those obtained with FGF19 in the same experimental set up (Figure 2G). Nevertheless, repression of *Cyp7a1* transcription was less efficient, and FGF15 expression did not significantly increase water intake nor reduced urine osmolality (Figure 2G). FGF15 shares only 53% of the amino acid sequence with FGF19 [39]; notably, FGF15 has an unpaired cysteine residue (Cys-135) that forms an intermolecular disulfide bridge to structure a homodimer. It has been suggested that this particularity leads to a diminished receptor activation and metabolic effects compared to FGF19 [37]. In summary, hepatic overexpression of FGF19 results in supra-physiological circulating biologically active FGF19, which in turn stimulates water intake, a remarkably robust and long-lasting phenotype.

3.3. FGF19 effect on the central nervous system

To test if the role of FGF19 in water homeostasis is central or peripheral, we performed an intraperitoneal injection of 2 mL of water to subject mice to an acute increase in water load. Cumulative urine excretion showed that the $FGF19^+$ mice displayed a similar response to water loading compared to control mice. This is in contrast with the increased urine output observed in $FGF19^+$ mice when given free access to water (Figure 3A, 206 μL $CI_{95\%}$ = [123; 290] for controls *vs* 433 μL $CI_{95\%}$ = [330; 535] for FGF19, p = 0.0013, and Figure 2C). These data suggest that FGF19 has no impact on water clearance but rather stimulates voluntary water intake, presumably via the implication of the central nervous system.

The phenotype we report is reminiscent of what has been described for FGF21, where pharmacologic administration of the hormone also increased water consumption in mice [29,30,40,41]. In a physiological context, FGF21 has been shown to stimulate water drinking in response to dehydration caused by metabolic stresses such as ketogenic diet or alcohol consumption [30]. FGF21 impact on water homeostasis is mediated in part by activation of the neurons of the paraventricular nucleus in the hypothalamus, through activation of FGFR1c/β-klotho signaling [30]. FGF19 has also been shown to exert effects on the central nervous system via FGFR1c/β-klotho signaling [11,42,43], suggesting that FGF19-mediated stimulation of water consumption might rely on the FGFR1c/β-klotho activation in the hypothalamus.

To test this hypothesis, we generated $FGF19^{\Delta CTD}$, a molecule in which the C-terminal region of FGF19 was removed (deletion of amino acids 178-216) as previously described [26] (Figure 3B). The C-terminal region is necessary for binding to β-klotho, in consequence $FGF19^{\Delta CTD}$ loses the ability to activate FGFR1c, but is still able to bind and activate FGFR4 in hepatocytes via heparin binding [26]. Hepatic overexpression of this mutant following hydrodynamic injection gave rise to similar plasma levels compared to wild-type FGF19 (mean: 12 ng/mL, $CI_{95\%}$ = [6.0; 18.0] ng/mL). It resulted in inhibition of hepatic *Cyp7a1* expression (Figure 3B), but had no effect on water intake (Figure 3B,

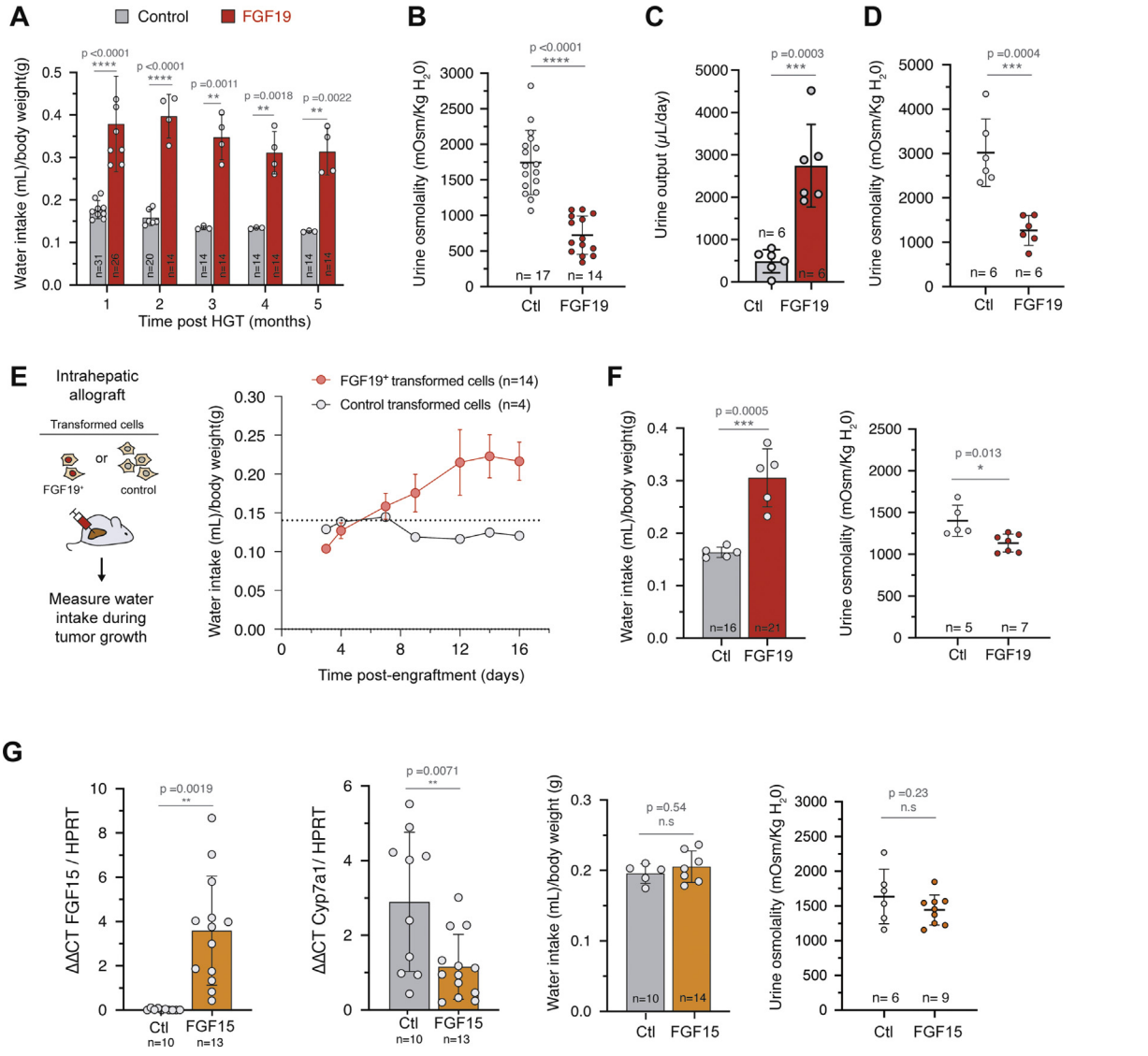

Figure 2: FGF19 increases water intake and urine output. A. Water consumption of control and FGF19+ female mice. The number of mice analyzed for each time point is indicated and each dot represents the mean value of an independent cage over one month. **B.** Urine osmolality of control and FGF19+ female mice at 3 months post HGT. **C.** Daily urine output in female mice housed in metabolic cages. **D.** Urine osmolality of control and FGF19+ female mice housed in metabolic cages. **E.** Daily water consumption of female mice following intrahepatic allograft of FGF19+ (MYC-sgTrp53-FGF19) and control (MYC-sgTrp53) cell lines. Mean water consumption is shown, corresponding to 14 mice (3 cages) or 4 mice (1 cage), as indicated. Dotted line represents the mean consumption of C57Bl/6J mice on the same period in the animal facility (n = 15). **F.** Effect of FGF19 overexpression on daily water intake and urine osmolality on male mice 1 month post HGT. **G.** qPCR quantification of FGF15 and Cyp7a1 mRNA (left panels) in livers of female mice injected with FGF15-BFP (FGF15) or BFP plasmid (control, Ctl). Daily water consumption and urine osmolality (right panels) of FGF15 or control female mice 1 month post HGT, normalized by the body weight. In (A–G): data are presented as mean ± SD. For water intake mesures, each dot represents the mean value of an independent cage with two to five mice. For all panels, unpaired t-test statistical significance is indicated. *p ≤ 0.05, **p < 0.01, ***p < 0.001, ****p < 0.0001. n. s: not significant.

0.17 mL/day/g body weight $CI_{95\%}$ = [0.16; 0.18] mL/day, and Supplementary Fig. 2). Thus, stimulation of water consumption by FGF19 is β-klotho dependent while activation of hepatic FGFR4 is not sufficient to elicit this phenotype. This is important because bile acids, the synthesis of which is repressed by the FGF19/FGFR4 pathway, have been proposed as regulators of hydric balance. Notably, it has been shown that inactivation of the bile acid nuclear receptor FXR leads to a decrease in urine osmolality [44] through the regulation of aquaporin water channel (aquaporin 2) in the renal collecting ducts. Our results from experiments with truncated FGF19 make it unlikely that bile acids are involved in the stimulation of water intake by FGF19.

Because FGF21 has also been described in the phenotype of sugar appetence [29], we submitted control, FGF19 and $FGF19^{\Delta CTD}$ mice to a two-bottle preference study between water and 3% sucrose. Strikingly, we observed the same phenotype as with FGF21, i.e. FGF19 overexpressing mice showed reduced appetence for 3% sucrose water (Figure 3C, at week1: 91% $CI_{95\%}$ = [83.7; 97.8] for controls *vs* 54% $CI_{95\%}$ = [37; 72] for FGF19, p = 0.005). Again, this effect was lost with the expression of the FGF19 mutant $FGF19^{\Delta CTD}$, unable to bind β-klotho and therefore to activate FGFR1c (Figure 3C). An alternative mechanism for FGF19 phenocopying the FGF21 effect would be that the former increases the latter's secretion. This is however not the

case, as measurements of FGF21 plasma levels indicated that FGF19 expression had no effect on the FGF21 levels (Figure 3D). Overall, we conclude that FGF19 effect on water homeostasis is central and independent of FGF21. It likely occurs through activation of FGFR1c/β-klotho in the hypothalamus.

3.4. HCC patients with high circulating FGF19 have reduced natremia

To explore if the effects of FGF19 on water homeostasis have a clinical relevance, we considered pathological conditions associated with supra-physiological concentrations of FGF19. A subset of patients with hepatocellular carcinoma (HCC) have increased FGF19 serum levels [22], and around 10% of tumors are characterized by the amplification of the FGF19 genomic locus [17,19]. In healthy subjects, FGF19 plasma levels range from 50 to 590 pg/mL [45]. To explore a potential effect on water homeostasis in patients with increased circulating levels of FGF19, we assayed FGF19 concentration in plasma from 173 HCC patients from the "Liverpool Cohort", held in the Montpellier University Hospital. Most patients were male (89%), had underlying cirrhosis (81%) and multifocal or advanced HCC stage (BCLC B, C or D stage, 73%). We defined three groups based on the result of the FGF19 ELISA assay (Figure 4A): "high FGF19" for the upper quartile ([FGF19] $>$ 603 pg/mL, 43 patients), "intermediate FGF19" for the middle quartiles ([FGF19] between 218 pg/mL and 603 pg/mL, 87 patients) and "low FGF19" for the lower quartile ([FGF19] $<$ 218 pg/mL, 43 patients). "High FGF19" group corresponded to supra-physiological concentrations based on the literature [1,45]. Interestingly, natremia of the "high FGF19" group was significantly lower than of the two other groups (Figure 4B, 140.1 mmol/L $Cl_{95\%}$ = [139.4; 140.8] for "low FGF19" *vs* 139.2 mmol/L $Cl_{95\%}$ = [138.5; 139.9] for "intermediate FGF19" *vs* 137.1 mmol/L $Cl_{95\%}$ = [136.2; 138] for "high FGF19", $p < 0.0001$). Values of natremia below 140 mmol/L are a major prognostic factor in patients with cirrhosis [32] and natremia is needed to establish the MELD-Na score, currently used to prioritize patients on the liver transplantation waiting list in the United States. It is therefore of particular interest that MELD Na score is significantly

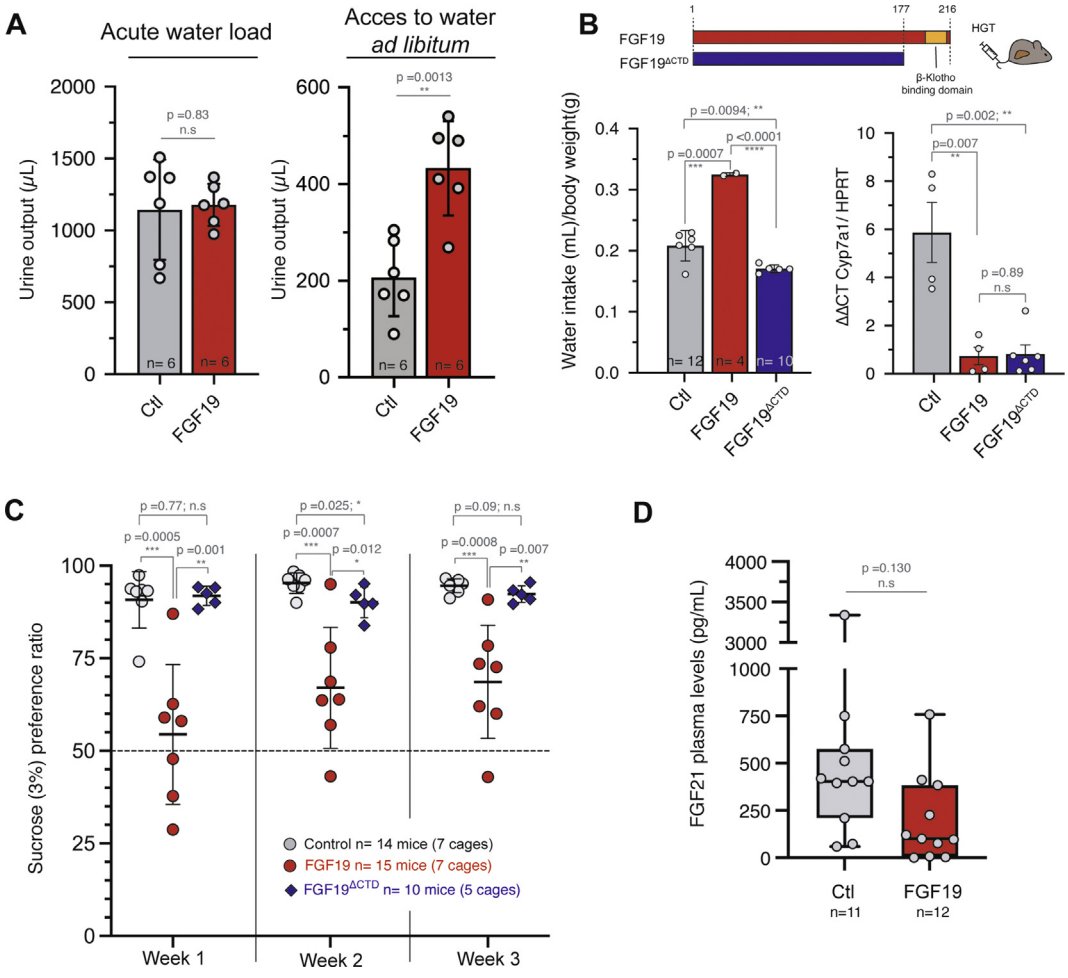

Figure 3: FGF19 regulates water homeostasis through central regulation. A. Urine output and urine osmolality 6 h after acute water load or free acces to water. n = 6 mice per group. **B.** Schematic diagram showing FGF19 and $FGF19^{\Delta CTD}$. The deleted sequence contains water consumption of female mice with hydrodynamic injection of control, FGF19, or $FGF19^{\Delta}$ (AA 1-177). Mean consumption over the first month after injection is shown. Each dot represents one cage with two animals. Total number of animals in each group is indicated. qPCR quantification of mRNA expression of Cyp7a1. Data are presented as mean ± SD, and unpaired Student's t-test p-values indicated. **C.** Sucrose (3%) preference ratio in double-bottle experiment. Experiments were carried out at least one month after the hydrodynamic injection. Each dot represents the mean of two to three measures over a week for a cage containing two animals. The total number of animals is indicated. **D.** FGF21 plasma levels determined by ELISA in control and FGF19 HGT mice. Number of animals is indicated. Data are presented as mean ± SD, and unpaired Student's t-test p-values indicated. *$p \leq 0.05$, **$p \leq 0.01$, ***$p \leq 0.001$, ****$p \leq 0.0001$. n. s: not significant. ***$p \leq 0.0001$. n. s: not significant.

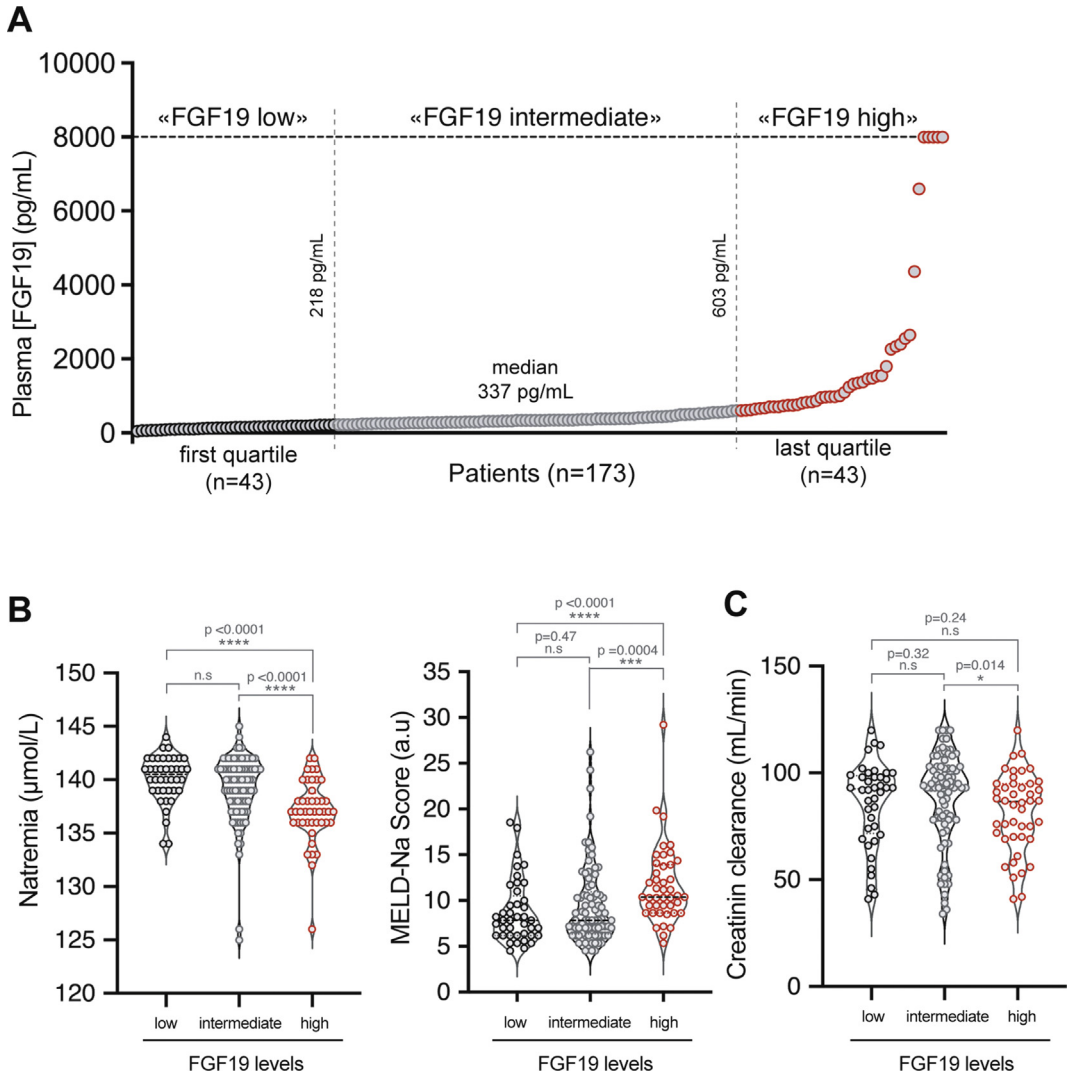

Figure 4: Increased FGF19 in hepatocellular carcinoma patients is associated with disturbances of the hydrosodic balance . A. Serum FGF19 distribution in a cohort of 173 patients with advanced HCC (FGF19 measured by ELISA). Median value and values at transitions between low, intermediate and high groups are indicated. **B.** Natremia (left panel) and MELD-Na score (right panel) in patients of the cohort according to the plasma FGF19 concentration **C.** Creatinin clearance in patients of the cohort according to the plasma FGF19 concentration. Mann Whitney test significance is indicated. *p $\leq$ 0.05, **p $\leq$ 0.01, ***p $\leq$ 0.001, ****p $\leq$ 0.0001. n. s: not significant.

higher in FGF19 high group compared to FGF19 low and intermediate groups. Our results are suggestive of an imbalance in the regulation of the sodium and water homeostasis, potentially via an increased water consumption in a context of effective hypovolemia in this cohort of predominantly cirrhotic patients. Of interest, this effect remains significant when subjects under diuretic treatment or with clinical ascites are excluded from the analysis (data not shown). Moreover, the natremia difference did not seem related to an impaired renal function in "FGF19 high" group (Figure 4C). Thus, our data from HCC patients with increased circulating FGF19 concentrations are consistent with an effect on water sodium balance in patients. Further work is required to establish if a reduction in natremia might have a prognostic value for FGF19-driven hepatocellular carcinoma. Finally, since FGF19 analogs are currently tested in several clinical trials, we suggest that it would be of interest to analyze the newly discovered FGF19 activity, specifically natremia and water intake, in response to these compounds.

4. CONCLUSIONS

Our study describes a novel biological function of FGF19, namely the increase in water intake and urine output caused by high levels of circulating FGF19. This phenotype involves a central regulation, likely through activation of FGFR1c/β-klotho in the hypothalamus, which indicates overlapping functions with FGF21. Importantly, FGF19 is overexpressed in a subset of HCCs and we show that patients with high circulating levels of FGF19 display a reduced natremia, suggestive of a hydrosodic balance disturbance. Since HCC arises mostly in patients with cirrhosis, a hormone inducing hyponatremia in this context has high clinical relevance, as it could trigger hepatic encephalopathy. Furthermore, it would be of interest to determine if the phenotype described in this report is also observed in patients with other tumor types (esophagus, breast, …) in which the FGF19 gene locus amplification has been described.

AUTHOR CONTRIBUTIONS

JUB: Conceptualization, Methodology, Investigation, Writing-original draft, Writing-review & editing; CC: Conceptualization, Investigation, Writing-review & editing; LM: Investigation; GD: Investigation; IG: Investigation; AD: Resources, Investigation; TT: Resources; EA: Supervision, Funding acquisition, Writing-review & editing; UH: Supervision, Funding acquisition, Writing-review & editing; DG: Conceptualization, Investigation, Visualization, Supervision, Funding acquisition, Writing-original draft, Writing-review & editing.

ACKNOWLEDGMENTS

We acknowledge Montpellier Biocampus facilities: the imaging facility (MRI), and the "Réseau d'Histologie Expérimentale de Montpellier" - RHEM facility, supported by SIRIC Montpellier Cancer (Grant INCa_Inserm_DGOS_12553), the European regional development foundation and the Occitanie region (FEDER-FSE 2014-2020 Languedoc Roussillon), for the histological analyses. We are grateful to zootechnicians of IGMM animal housing facility, Cédric Orféo, Eve Lasserre, Zoé Lebrere, for their work. We thank Emmanuel Vignal for the osmometer and Anne-Dominique Lajoix for allowing access to metabolic cages. We thank members of our lab for helpful discussions and comments. We acknowledge Montpellier University Hospital research staff and patients included in the Liverpool cohort. This work was funded by EVA-Plan cancer INSERM THE, the Association Française pour l'Etude du Foie (AFEF), and supported by SIRIC Montpellier Cancer Grant INCa_Inserm_DGOS_12553. The funders had no role in study design, data collection and analysis or publication process.

CONFLICT OF INTEREST

The authors declare no conflict of interest.

APPENDIX A. SUPPLEMENTARY DATA

Supplementary data to this article can be found online at https://doi.org/10.1016/j.molmet.2022.101483.

REFERENCES

[1] Angelin, B., Larsson, T.E., Rudling, M., 2012. Circulating fibroblast growth factors as metabolic regulators - a critical appraisal. Cell Metabolism 16(6): 693–705. https://doi.org/10.1016/j.cmet.2012.11.001.

[2] Gadaleta, R.M., Moschetta, A., 2019. Metabolic Messengers: fibroblast growth factor 15/19. Nature Metabolism 1(6):588–594. https://doi.org/10.1038/s42255-019-0074-3.

[3] Inagaki, T., Choi, M., Moschetta, A., Peng, L., Cummins, C.L., McDonald, J.G., et al., 2005. Fibroblast growth factor 15 functions as an enterohepatic signal to regulate bile acid homeostasis. Cell Metabolism 2(4):217–225. https://doi.org/10.1016/j.cmet.2005.09.001.

[4] Schaap, F.G., van der Gaag, N.A., Gouma, D.J., Jansen, P.L.M., 2009. High expression of the bile salt-homeostatic hormone fibroblast growth factor 19 in the liver of patients with extrahepatic cholestasis. Hepatology 49(4):1228–1235. https://doi.org/10.1002/hep.22771.

[5] Wunsch, E., Milkiewicz, M., Wasik, U., Trottier, J., Kempialska-Podhorodecka, A., Elias, E., et al., 2015. Expression of hepatic fibroblast growth factor 19 is enhanced in primary biliary cirrhosis and correlates with severity of the disease. Scientific Reports 5(March):1–13. https://doi.org/10.1038/srep13462.

[6] Hasegawa, Y., Kawai, M., Bessho, K., Yasuda, K., Ueno, T., Satomura, Y., et al., 2019. CYP7A1 expression in hepatocytes is retained with upregulated fibroblast growth factor 19 in pediatric biliary atresia. Hepatology Research 49(3):314–323. https://doi.org/10.1111/hepr.13245.

[7] Suzuki, M., Uehara, Y., Motomura-Matsuzaka, K., Oki, J., Koyama, Y., Kimura, M., et al., 2008. βklotho is required for fibroblast growth factor (FGF) 21 signaling through FGF receptor (FGFR) 1c and FGFR3c. Molecular Endocrinology 22(4):1006–1014. https://doi.org/10.1210/me.2007-0313.

[8] Wu, X., Ge, H., Lemon, B., Vonderfecht, S., Weiszmann, J., Hecht, R., et al., 2010. FGF19-induced hepatocyte proliferation is mediated through FGFR4 activation. Journal of Biological Chemistry 285(8):5165–5170. https://doi.org/10.1074/jbc.M109.068783.

[9] Wu, A.L., Coulter, S., Liddle, C., Wong, A., Eastham-Anderson, J., French, D.M., et al., 2011. FGF19 regulates cell proliferation, glucose and bile acid metabolism via FGFR4-dependent and independent pathways. PLoS One 6(3). https://doi.org/10.1371/journal.pone.0017868.

[10] Lan, T., Morgan, D.A., Rahmouni, K., Sonoda, J., Fu, X., Burgess, S.C., et al., 2017. FGF19, FGF21, and an FGFR1/β-klotho-activating antibody act on the nervous system to regulate body weight and glycemia. Cell Metabolism 26(5): 709–718.e3. https://doi.org/10.1016/j.cmet.2017.09.005.

[11] Perry, R.J., Lee, S., Ma, L., Zhang, D., Schlessinger, J., Shulman, G.I., 2015. FGF1 and FGF19 reverse diabetes by suppression of the hypothalamic-pituitary-adrenal axis. Nature Communications 6:1–10. https://doi.org/10.1038/ncomms7980.

[12] Degirolamo, C., Sabbà, C., Moschetta, A., 2016. Therapeutic potential of the endocrine fibroblast growth factors FGF19, FGF21 and FGF23. Nature Reviews Drug Discovery 15(1):51–69. https://doi.org/10.1038/nrd.2015.9.

[13] Harrison, S.A., Rinella, M.E., Abdelmalek, M.F., Trotter, J.F., Paredes, A.H., Arnold, H.L., et al., 2018. NGM282 for treatment of non-alcoholic steatohepatitis: a multicentre, randomised, double-blind, placebo-controlled, phase 2 trial. The Lancet 391(10126):1174–1185. https://doi.org/10.1016/S0140-6736(18)30474-4.

[14] Harrison, S.A., Rossi, S.J., Paredes, A.H., Trotter, J.F., Bashir, M.R., Guy, C.D., et al., 2020. NGM282 improves liver fibrosis and histology in 12 Weeks in patients with nonalcoholic steatohepatitis. Hepatology 71(4):1198–1212. https://doi.org/10.1002/hep.30590.

[15] Mayo, M.J., Wigg, A.J., Leggett, B.A., Arnold, H., Thompson, A.J., Weltman, M., et al., 2018. NGM 282 for treatment of patients with primary biliary cholangitis: a multicenter, randomized, double-blind, placebo-controlled trial. Hepatology Communications 2(9):1037–1050. https://doi.org/10.1002/hep4.1209.

[16] Hirschfield, G.M., Chazouillères, O., Drenth, J.P., Thorburn, D., Harrison, S.A., Landis, C.S., et al., 2019. Effect of NGM282, an FGF19 analogue, in primary sclerosing cholangitis: a multicenter, randomized, double-blind, placebo-controlled phase II trial. Journal of Hepatology 70(3):483–493. https://doi.org/10.1016/j.jhep.2018.10.035.

[17] Sawey, E.T., Chanrion, M., Cai, C., Wu, G., Zhang, J., Zender, L., et al., 2011. Identification of a therapeutic strategy targeting amplified FGF19 in liver cancer by oncogenomic screening. Cancer Cell 19(3):347–358. https://doi.org/10.1016/j.ccr.2011.01.040.

[18] Wang, K., Lim, H.Y., Shi, S., Lee, J., Deng, S., Xie, T., et al., 2013. Genomic landscape of copy number aberrations enables the identification of oncogenic drivers in hepatocellular carcinoma. Hepatology 58(2):706–717. https://doi.org/10.1002/hep.26402.

[19] Schulze, K., Imbeaud, S., Letouzé, E., Alexandrov, L.B., Calderaro, J., Rebouissou, S., et al., 2015. Exome sequencing of hepatocellular carcinomas identifies new mutational signatures and potential therapeutic targets. Nature Genetics 47(5):505–511. https://doi.org/10.1038/ng.3252.

[20] Caruso, S., Calatayud, A.L., Pilet, J., La Bella, T., Rekik, S., Imbeaud, S., et al., 2019. Analysis of liver cancer cell lines identifies agents with likely efficacy against hepatocellular carcinoma and markers of response. Gastroenterology 157(3):760–776. https://doi.org/10.1053/j.gastro.2019.05.001.

[21] Hatlen, M.A., Schmidt-Kittler, O., Sherwin, C.A., Rozsahegyi, E., Rubin, N., Sheets, M.P., et al., 2019. Acquired on-target clinical resistance validates fgfr4 as a driver of hepatocellular carcinoma. Cancer Discovery 9(12):1686–1695. https://doi.org/10.1158/2159-8290.CD-19-0367.

[22] Maeda, T., Kanzaki, H., Chiba, T., Ao, J., Kanayama, K., Maruta, S., et al., 2019. Serum fibroblast growth factor 19 serves as a potential novel biomarker for hepatocellular carcinoma. BMC Cancer 19(1):1088. https://doi.org/10.1186/s12885-019-6322-9.

[23] Kim, R.D., Sarker, D., Meyer, T., Yau, T., Macarulla, T., Park, J.W., et al., 2019. First-in-human phase i study of fisogatinib (BLU-554) validates aberrant FGF19 signaling as a driver event in hepatocellular carcinoma. Cancer Discovery 9(12):1696–1707. https://doi.org/10.1158/2159-8290.CD-19-0555.

[24] Bartz, R., Fukuchi, K., Ohtsuka, T., Lange, T., Gruner, K., Watanabe, I., et al., 2019. Preclinical development of U3-1784, a novel FGFR4 antibody against cancer, and avoidance of its on-target toxicity. Molecular Cancer Therapeutics 18(10):1832–1843. https://doi.org/10.1158/1535-7163.MCT-18-0048.

[25] Gadaleta, R.M., Moschetta, A., 2021. Dark and bright side of targeting the fibroblast growth factor receptor 4 in the liver. Journal of Hepatology. https://doi.org/10.1016/j.jhep.2021.07.029.

[26] Wu, X., Ge, H., Lemon, B., Weiszmann, J., Gupte, J., Hawkins, N., et al., 2009. Selective activation of FGFR4 by an FGF19 variant does not improve glucose metabolism in ob/ob mice. Proceedings of the National Academy of Sciences of the United States of America 106(34):14379–14384. https://doi.org/10.1073/pnas.0907812106.

[27] Zhang, G., Vargo, D., Budker, V., Armstrong, N., Knechtle, S., Wolff, J.A., 1997. Expression of naked plasmid DNA injected into the afferent and efferent vessels of rodent and dog livers. Human Gene Therapy 8(15):1763–1772. https://doi.org/10.1089/hum.1997.8.15-1763.

[28] Liu, F., Song, Y., Liu, D., 1999. Hydrodynamics-based transfection in animals by systemic administration of plasmid DNA. Gene Therapy 6(7):1258–1266. https://doi.org/10.1038/sj.gt.3300947.

[29] Talukdar, S., Owen, B.M., Song, P., Hernandez, G., Zhang, Y., Zhou, Y., et al., 2016. FGF21 regulates sweet and alcohol preference. Cell Metabolism 23(2):344–349. https://doi.org/10.1016/j.cmet.2015.12.008.

[30] Song, P., Zechner, C., Hernandez, G., Cánovas, J., Xie, Y., Sondhi, V., et al., 2018. The hormone FGF21 stimulates water drinking in response to ketogenic diet and alcohol. Cell Metabolism 27(6):1338–1347.e4. https://doi.org/10.1016/j.cmet.2018.04.001.

[31] Bidault-Jourdainne, V., Merlen, G., Glénisson, M., Doignon, I., Garcin, I., Péan, N., et al., 2021. TGR5 controls bile acid composition and gallbladder function to protect the liver from bile acid overload. JHEP Reports 3(2):100214. https://doi.org/10.1016/j.jhepr.2020.100214.

[32] Kim, W.R., Biggins, S.W., Kremers, W.K., Wiesner, R.H., Kamath, P.S., Benson, J.T., et al., 2008. Hyponatremia and mortality among patients on the liver-transplant waiting list. New England Journal of Medicine 359(10):1018–1026. https://doi.org/10.1056/nejmoa0801209.

[33] Zhang, G., Budker, V., Wolff, J.A., 1999. High levels of foreign gene expression in hepatocytes after tail vein injections of naked plasmid DNA. Human Gene Therapy 10(10):1735–1737. https://doi.org/10.1089/10430349950017734.

[34] Fu, L., John, L.M., Adams, S.H., Yu, X.X., Tomlinson, E., Renz, M., et al., 2004. Fibroblast growth factor 19 increases metabolic rate and reverses dietary and leptin-deficient diabetes. Endocrinology 145(6):2594–2603. https://doi.org/10.1210/en.2003-1671.

[35] Tomlinson, E., Fu, L., John, L., Hultgren, B., Huang, X., Renz, M., et al., 2002. Transgenic mice expressing human fibroblast growth factor-19 display increased metabolic rate and decreased adiposity. Endocrinology 143(5):1741–1747. https://doi.org/10.1210/endo.143.5.8850.

[36] Benoit, B., Meugnier, E., Castelli, M., Chanon, S., Vieille-Marchiset, A., Durand, C., et al., 2017. Fibroblast growth factor 19 regulates skeletal muscle mass and ameliorates muscle wasting in mice. Nature Medicine 23(8):990–996. https://doi.org/10.1038/nm.4363.

[37] Zhou, M., Luo, J., Chen, M., Yang, H., Learned, R.M., DePaoli, A.M., et al., 2017. Mouse species-specific control of hepatocarcinogenesis and metabolism by FGF19/FGF15. Journal of Hepatology 66(6):1182–1192. https://doi.org/10.1016/j.jhep.2017.01.027.

[38] Nicholes, K., Guillet, S., Tomlinson, E., Hillan, K., Wright, B., Frantz, G.D., et al., 2002. A mouse model of hepatocellular carcinoma: ectopic expression of fibroblast growth factor 19 in skeletal muscle of transgenic mice. American Journal Of Pathology 160(6):2295–2307. https://doi.org/10.1016/S0002-9440(10)61177-7.

[39] Nishimura, T., Utsunomiya, Y., Hoshikawa, M., Ohuchi, H., Itoh, N., 1999. Structure and expression of a novel human FGF, FGF-19, expressed in the fetal brain. Biochimica et Biophysica Acta (BBA) - Gene Structure and Expression 1444(1):148–151. https://doi.org/10.1016/S0167-4781(98)00255-3.

[40] Camporez, J.P.G., Jornayvaz, F.R., Petersen, M.C., Pesta, D., Guigni, B.A., Serr, J., et al., 2013. Cellular mechanisms by which FGF21 improves insulin sensitivity in male mice. Endocrinology 154(9):3099–3109. https://doi.org/10.1210/en.2013-1191.

[41] Turner, T., Chen, X., Zahner, M., Opsahl, A., DeMarco, G., Boucher, M., et al., 2018. FGF21 increases water intake, urine output and blood pressure in rats. PLoS One 13(8). https://doi.org/10.1371/journal.pone.0202182.

[42] Marcelin, G., Jo, Y.H., Li, X., Schwartz, G.J., Zhang, Y., Dun, N.J., et al., 2014. Central action of FGF19 reduces hypothalamic AGRP/NPY neuron activity and improves glucose metabolism. Molecular Metabolism 3(1):19–28. https://doi.org/10.1016/j.molmet.2013.10.002.

[43] Liu, S., Marcelin, G., Blouet, C., Jeong, J.H., Jo, Y.H., Schwartz, G.J., et al., 2018. A gut–brain axis regulating glucose metabolism mediated by bile acids and competitive fibroblast growth factor actions at the hypothalamus. Molecular Metabolism 8(December 2017):37–50. https://doi.org/10.1016/j.molmet.2017.12.003.

[44] Zhang, X., Huang, S., Gao, M., Liu, J., Jia, X., Han, Q., et al., 2014. Farnesoid X receptor (FXR) gene deficiency impairs urine concentration in mice. Proceedings of the National Academy of Sciences 111(6):2277–2282. https://doi.org/10.1073/pnas.1323977111.

[45] Lundåsen, T., Gälman, C., Angelin, B., Rudling, M., 2006. Circulating intestinal fibroblast growth factor 19 has a pronounced diurnal variation and modulates hepatic bile acid synthesis in man. Journal of Internal Medicine 260(6):530–536. https://doi.org/10.1111/j.1365-2796.2006.01731.x.

